SIMULATIONS OF INDIUM ARSENIDE / GALLIUM ANTIMONIDE SUPERLATTICE BARRIER BASED THERMOPHOTOVOLTAIC CELLS

Dante DeMeo[a], Abigail Licht[a], Corey Shemelya[a], J.-M. Masur[b], R. Rehm[b], M. Walther[b], Thomas E. Vandervelde[a]
[a]*Renewable Energy and Applied Photonics Laboratories, Department of Electrical and Computer Engineering, Tufts University, 161 College Avenue, Medford, MA 02155*
[b]*Fraunhofer-Institut für Angewandte Festkörperphysik, Tullastraße 72, 79108 Freiburg, Germany*

ABSTRACT: Thermophotovoltaic (TPV) cells are semiconductor devices which convert radiated heat directly into electricity. This work investigates extending the operational wavelength of such devices into the long-wavelength infrared regime. Specifically, this work explores the use a barrier layer inserted into a p-n junction to suppress recombination pathways. Dark current simulations have been performed comparing a heterojunction barrier case with a typical p-n junction. Doping levels were varied to adjust the size of the space charge region of the junction and simulate the effect of different barrier widths within the depletion region.
Keywords: Thermophotovoltaics, Recombination, Heterojunction, III-V Semiconductors

1 INTRODUCTION AND BACKGROUND

Thermophotovoltaic (TPV) cells are a technology which converts radiated heat directly into electricity. TPV devices operate using the photovoltaic effect, just as solar panels do, however TPV devices focus on the infrared regime of the electromagnetic spectrum. TPV systems often use different forms of spectral control, such as an emitter and filter (see Fig. 1), to increase the efficiency of the TPV cell and system. Other benefits of this system include the decoupling of the radiation source and the photovoltaic diode, allowing for greater material freedom in the TPV cell. The system also allows photon recycling as a percent of the reflected photons are re-absorbed and subsequently re-emitted by the emitter component. The spectral control as well as the narrow band gaps typically used in TPV devices, allow TPV to utilize a myriad of heat sources to create energy.

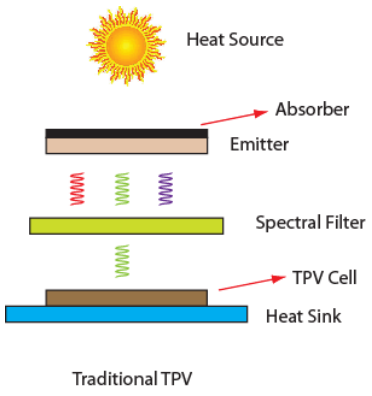

Figure 1: Traditional TPV configuration

This research aims to extend the operational wavelengths of TPV further into the infrared. However, at these wavelengths, exciton recombination within the TPV cell significantly reduces device performance. To reduce recombination events, a unipolar, or monovalent, barrer is to be epitaxially grown into the TPV cell. Originally proposed for use in photodetectors [1], this barrier is designed to block only one carrier, and can exist in either the valence band or the conduction band. The unipolar barrier has shown considerable success with photodetectors [2]–[8] however, this work proposes to impliment the barrier in a photovoltaic device in order to suppress recombination pathways such as Shockley-Reed-Hall (SRH). SRH recombination occurs in the space charge, or depletion, region of a p-n junction due to generation-recombination centers, also called traps.[9] In order to mittigate this recombination pathway, the unipolar barrier, consisting of a wider-bandgap material, is placed between the p and n materials in a pn junction. The addition of the wider bandgap increases the energy needed for a carrier to recombine at the mid-level trap, thus decreasing the probability of SRH recombination.

Previous work has investigated using unipolar barriers with bulk materials such as gallium antimonide (GaSb) [10] and indium arsenide antimonide [11] in barrier based TPV cells; however, our work uses indium asenide (InAs) / GaSb type-II strained layer superlattices (SLS) [12][13][14]. These structures enable an effective bandgaps narrower than is possible with most bulk materials, which in turn allow TPV devices to harvest longer wavelength radiation from lower temperature heat sources. Type-II SLS create these narrower bandgap devices through the creation of minibands in periodic quantum wells.

Unipolar barriers have been shown to help suppress the components of dark current, such as surface leakage currents, trap-assisted tunneling, and SRH recombination[15], [16], however none have investigated their use for TPV cells.

2 SIMULATION DETAILS

The dark current was estimated using two components: diffusion current and generation-recombination (G-R) current. Contributions from surface leakage current and tunneling current were not taken into account in this study, although will be implemented in future iterations of our simulation model. Diffusion current occurs due to the change in concentration of the charge carriers, and is alternatively referred to as saturation current when under reverse bias. G-R current describes the generation and recombination of carriers within the space charge region (SCR). Often G-R recombination is caused by traps at the mid-level of the bandgap. These traps facilitate recombination, increasing G-R current, by providing a lower energy pathway for carriers to recombine.

A unipolar barrier diode heterojunction case was examined alongside a typical p-n homojunction as a control. Diffusion current for a homojunction was calculated according to Equation 1, while the heterojunction case can be found in Equation 2.

$$I_{diff} = n_i^2 \sqrt{qk_BT} \cdot \left(\frac{1}{p} \sqrt{\frac{\mu_n}{\tau_n}} + \frac{1}{n} \sqrt{\frac{\mu_p}{\tau_p}} \right) \cdot \left(e^{\frac{qV_d}{k_BT}} - 1 \right) \quad \textbf{Eq. 1}$$

$$I_{diff\_hetero} = \sqrt{qk_BT} \cdot \left(\frac{n_{iN}^2}{p} \sqrt{\frac{\mu_{np}}{\tau_{np}}} + \frac{n_{ip}^2}{n} \sqrt{\frac{\mu_{pN}}{\tau_{pN}}} \right) \cdot \left(e^{\frac{qV_d}{k_BT}} - 1 \right) \quad \textbf{Eq. 2}$$

In these equations, q is the electron charge, k_B is the boltzman constant, μ and τ are the carrier mobility and carrier lifetime respectively with the subscripts depicting different locations in the device, T represents temperature, V_d is the built-in voltage of the diode minus any applied voltage, and the number of intrinsic carriers, n_i, is determined using Equation 3.

$$n_i = \sqrt{N_C N_V} \exp\left(\frac{-E_g}{k_BT} \right) \quad \textbf{Eq. 3}$$

The effective conduction band density of states, Nc, is given in Equation 4, and the effective valence band density of states, Nv, is given in Equation 5.

$$N_C = 2 * \left(\frac{2\pi * m_e * k_B * T}{h^2} \right)^{3/2} \quad \textbf{Eq. 4}$$

$$N_V = 2 * \left(\frac{2\pi * m_h * k_B * T}{h^2} \right)^{3/2} \quad \textbf{Eq. 5}$$

m_e is the effective mass of an electron, m_h is the effective hole mass, and h is the Planck constant. The generation-recombination current is calculated according to Equation 6 for the homojunction case and Equation 7 for the heterojunction case.

$$I_{GR} = q \cdot \int_{-x_p}^{x_n} G(x)dx \qquad G(x) \propto n_i \quad \textbf{Eq. 6}$$

The G-R current shown in Equation 6 is simply the integral of the trap-assisted recombination rate G(x) over the depletion region of width x. The heterojunction case is the same process; however, it splits the calculation into two parts: one integral for the p-type material, and another for the n-type.

$$I_{GR\_hetero} = q \cdot \int_{-x_p}^{0} G_p(x)dx + q \cdot \int_{0}^{x_N} G_N(x)dx \quad \textbf{Eq. 7}$$

3 SIMULATION RESULTS

The equations presented in the previous section were then used to simulate the TPV cell using Mathematica. The bandstructure of the non-barrier, homojunction control can be seen on the left in Figure 2, while the barrier case can be seen on the right. This figure depicts the space charge region (SCR) contained within the yellow bars and how much of it the barrier occupies.

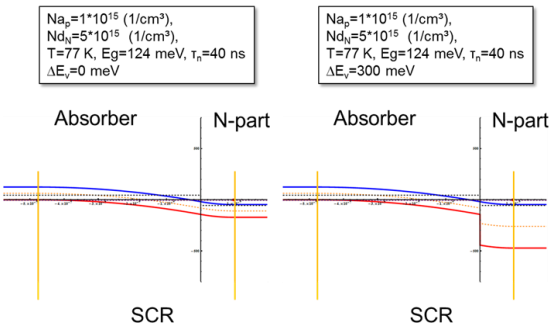

Figure 2: Band-alignment and parameters for **Left:** a homojunction, non-barrier case and **Right:** a heterojunction, barrier case.

Figure 3 examines the diffusion and G-R current from the two band-alignments depicted in Figure 2. The dashed lines indicate the dark current components from a non-barrier device, whereas the solid lines indicate the dark current components from a barrier device. The simulation parameters are listed in the inset.

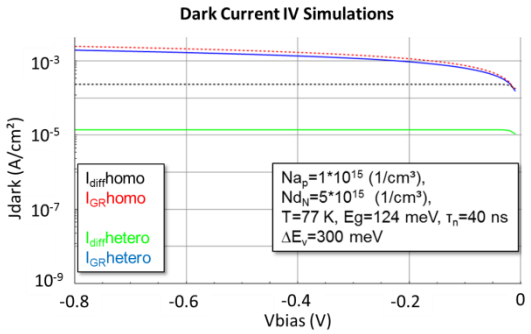

Figure 3: Dark current I-V simulation for the case presented in Figure 2. The black and red dashed lines are the contributions from diffusion and G-R currents respectively for a non-barrier device. The green and blue solid lines represent the contributions from diffusion and G-R currents respectively for a barrier device. The simulation parameters are listed in the inset.

Figure 4 compares the diffusion and G-R current for a similar scenario with alternative doping concentrations. The increase in absorber doping decreases the extent of band curvature in the absorber, while increasing the extent of it in the barrier. By moving more of the band curvature to the higher bandgap barrier region we further decrease the recombination rates. The dashed lines indicate the dark current components from a non-barrier device, whereas the solid lines indicate the dark current components from a barrier device. The specific parameters are listed in the inset

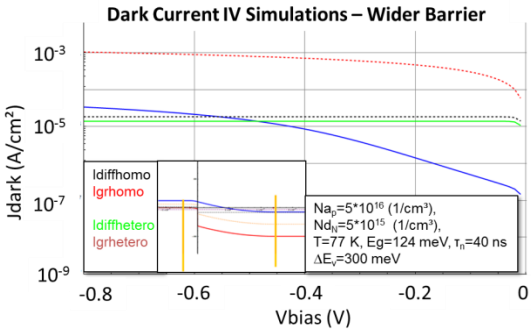

Figure 4: Dark current I-V simulation for a barrier that occupies the majority of the SCR. The black and red dashed lines are the contributions from diffusion and G-R currents respectively for a non-barrier device. The green and blue solid lines represent the contributions from diffusion and G-R currents respectively for a barrier device. The inset graph shows the amount of the SCR occupied by the barrier.

4 CONCLUSIONS

The unipolar barrier simulations have shown that introducing a barrier in the space charge region of a photovoltaic device decreases the components of dark current by several orders of magnitude. Specifically, a decrease of approximately two orders of magnitude in Schockley-Reed-Hall generation-recombination events was demonstrated when the absorber doping is set so that the barrier occupies most of the SCR. Also, a reduction in diffusion current by approximately one order of magnitude was shown when the barrier occupies only a quarter of the SCR. These simulations also showed that an increase in absorber doping pushes the bandbending into the barrier layer, minimizing recombination.

It should be noted that the introduction of a barrier presents a performance tradeoff, because the SCR is the optimum region to absorb carriers due to the built-in voltage. The authors believe, that this trade-off will provide an increased benifit for long-wavelength devices due to the increased effect of SRH recombination rates associated with narrow-bandgap devices.

These simulation results are promising; however, physical device fabrication and testing is necessary to confirm these findings. MBE grown devices have been designed and are presently being fabricated. As such, physical testing is forthcoming for this work. We are also working to improve our model accuracy by taking into account other components of dark current such as surface leakage and tunneling current as well as factors such as the effect of higher temperatures on doping concentration.

5 ACKNOWELEDGEMENTS

This material is based upon work supported by the National Science Foundation Graduate Research Fellowship under Grant No. DGE-0806676. Funding from the NSF has also been provided through grant ECCS-1055203.

6 REFERENCES

[1] S. Maimon and G. W. Wicks, “nBn detector, an infrared detector with reduced dark current and higher operating temperature,” *Appl. Phys. Lett.*, vol. 89, no. 15, p. 151109, Oct. 2006.

[2] A. Khoshakhlagh, J. B. Rodriguez, E. Plis, G. D. Bishop, Y. D. Sharma, H. S. Kim, L. R. Dawson, and S. Krishna, “Bias dependent dual band response from InAs/Ga(In)Sb type II strain layer superlattice detectors,” *Appl. Phys. Lett.*, vol. 91, no. 26, p. 263504, 2007.

[3] C. Downs and T. E. Vandervelde, “Progress in infrared photodetectors since 2000.,” *Sensors (Basel).*, vol. 13, no. 4, pp. 5054–98, Jan. 2013.

[4] A. Barve, J. Shao, Y. D. Sharma, T. E. Vandervelde, K. Sankalp, S. J. Lee, S. K. Noh, and S. Krishna, “Resonant Tunneling Barriers in Quantum Dots-in-a-Well Infrared Photodetectors,” *IEEE J. Quantum Electron.*, vol. 46, no. 7, pp. 1105–1114, Jul. 2010.

[5] R. V. Shenoi, J. Rosenberg, T. E. Vandervelde, O. J. Painte, and S. Krishna, “Multispectral Quantum Dots-in-a-Well Infrared Detectors Using Plasmon Assisted Cavities,” *IEEE J. Quantum Electron.*, vol. 46, no. 7, pp. 1051–1057, Jul. 2010.

[6] T. E. Vandervelde and S. Krishna, “Progress and prospects for quantum dots in a well infrared photodetectors.,” *J. Nanosci. Nanotechnol.*, vol. 10, no. 3, pp. 1450–60, Mar. 2010.

[7] P. Vines, C. H. Tan, J. P. R. David, R. S. Attaluri, T. E. Vandervelde, and S. Krishna, “Multiple stack quantum dot infrared photodetectors,” in *SPIE Europe Security and Defence*, 2008, p. 71130J–71130J–7.

[8] J. R. Andrews, S. R. Restaino, T. E. Vandervelde, J. S. Brown, Y. D. Sharma, S. J. Lee, S. W. Teare, A. Reisinger, M. Sundaram, and S. Krishna, “Comparison of Long-Wave Infrared Quantum-Dots-in-a-Well and Quantum-Well Focal Plane Arrays,” *IEEE Trans. Electron Devices*, vol. 56, no. 3, pp. 512–516, Mar. 2009.

[9] C. Sah, R. Noyce, and W. Shockley, “Carrier Generation and Recombination in P-N Junctions and P-N Junction Characteristics,” *Proc. IRE*, vol. 45, no. 9, pp. 1228–1243, 1957.

[10] D. F. DeMeo and T. E. Vandervelde, “Simulations of Gallium Antimonide (GaSb) p-B-n Thermophotovoltaic Cells,” *MRS Proc.*, vol. 1329, no. -1, Jan. 2011.

[11] D. F. DeMeo and T. E. Vandervelde, "Simulations of indium arsenide antimonide (InAs0.91Sb0.09) monovalent barrier-based thermophotovoltaic cells," *Photovoltaic Specialists Conference (PVSC), 2011 37th IEEE*. pp. 2047–2049, 2011.

[12] R. Rehm, M. Masur, J. Schmitz, V. Daumer, J. Niemasz, T. Vandervelde, D. DeMeo, W. Luppold, M. Wauro, A. Wörl, F. Rutz, R. Scheibner, J. Ziegler, and M. Walther, "InAs/GaSb superlattice infrared detectors," *Infrared Phys. Technol.*, vol. 59, pp. 6–11, Jul. 2013.

[13] C. Shemelya and T. E. Vandervelde, "Comparison of Photonic-Crystal-Enhanced Thermophotovoltaic Devices With and Without a Resonant Cavity," *J. Electron. Mater.*, vol. 41, no. 5, pp. 928–934, Apr. 2012.

[14] D. F. DeMeo and T. E. Vandervelde, "Cryogenic thermal simulator for testing low temperature thermophotovoltaic cells," *J. Vac. Sci. Technol. B Microelectron. Nanom. Struct.*, vol. 29, no. 3, p. 031401, Apr. 2011.

[15] G. R. Savich, J. R. Pedrazzani, S. Maimon, and G. W. Wicks, "Suppression of surface leakage currents using molecular beam epitaxy-grown unipolar barriers," *J. Vac. Sci. Technol. B Microelectron. Nanom. Struct.*, vol. 28, no. 3, p. C3H18, Apr. 2010.

[16] G. R. Savich, J. R. Pedrazzani, D. E. Sidor, S. Maimon, and G. W. Wicks, "Dark current filtering in unipolar barrier infrared detectors," *Appl. Phys. Lett.*, vol. 99, no. 12, p. 121112, Sep. 2011.